

# Design of the Adaptive Optics Systems for GMT

Michael Lloyd-Hart, Roger Angel, N. Mark Milton, Matt Rademacher, and Johanan Codona  
Steward Observatory, The University of Arizona, Tucson, AZ 85721

## ABSTRACT

The Giant Magellan Telescope (GMT) includes adaptive optics (AO) as an integral component of its design. Planned scientific applications of AO span an enormous parameter space: wavelengths from 1 to 25  $\mu\text{m}$ , fields of view from 1 arcsec to 8 arcmin, and contrast ratio as high as  $10^9$ . The integrated systems are designed about common core elements. The telescope's Gregorian adaptive secondary mirror, with seven segments matched to the primary mirror segments, will be used for wavefront correction in all AO modes, providing for high throughput and very low background in the thermal infrared. First light with AO will use wavefront reconstruction from a constellation of six continuous-wave sodium laser guide stars to provide ground-layer correction over 8 arcmin and diffraction-limited correction of small fields. Natural guide stars will be used for classical AO and high contrast imaging. The AO system is configured to feed both the initial instrument suite and ports for future expansion.

**Keywords:** Adaptive optics, tomography, extremely large telescopes, Giant Magellan Telescope

## 1. INTRODUCTION

The Giant Magellan Telescope (GMT) project, described at this symposium by Johns,<sup>1</sup> is a collaboration of nine partner institutions to build a 25 m next-generation telescope. The design for GMT's adaptive optics (AO) systems were presented as part of the telescope's Conceptual Design Review in February 2006. We summarize in this paper the design and anticipated performance of the AO, with the exception of the very high contrast (ExAO) system, which is reported on separately.<sup>2</sup>

### 1.1. Goals for the AO system

The promise of an extremely large telescope (ELT) with AO, combining sharper resolution at the diffraction limit with a huge collecting area, is obvious. But realizing the promise in practice will require extraordinary care. Our expectation is that very high resolution can be achieved, and with a Strehl ratio of 40% for H band images even at the Galactic poles when the guide star is 1 arcmin off axis. The GMT's large aperture gives inherently better sky access than present 8 m telescopes; thus adaptive correction will be a powerful tool for the general observer.

The primary goal of AO is the correction of atmospheric blurring to recover images with the telescope's diffraction-limited beam profile. The resulting unprecedented sensitivity and resolution of the GMT are illustrated by the modeled H $\alpha$  image in Figure 1 of a starburst galaxy at  $z = 1.4$ , in a 1 hour, narrow-band exposure at 1.58  $\mu\text{m}$ . AO corrected images from GMT with high Strehl ratio in the thermal infrared will realize the ideal diffraction-limited profile in practice, with access to most of the sky and with no compromise of the thermal infrared background.

A prerequisite for general access to the sky is the use of laser guide stars (LGS) for wavefront sensing. The power of LGS for science programs is being realized at the Keck II telescope,<sup>3</sup> where a single sodium beacon is now in routine use. For ELTs, where the cone effect from a single LGS is prohibitive, multiple beacons must be used to enable a tomographic view of the aberration. For the GMT, six sodium lasers will be projected in a small-angle constellation from a common launch telescope. The tomographic solution driving an adaptive secondary mirror will correct the wavefront to the diffraction limit in a technique called laser tomography adaptive optics (LTAO).

The sky coverage is potentially better than for present 8 m systems for two reasons. One is that the anisoplanatic error in tip-tilt measurement made from a field star at given radius decreases with aperture, even faster than the decrease in diffraction width. For typical atmospheric conditions, the RMS differential motion projected for the diffraction limited GMT rises to only  $\sim 5$  milliarcseconds (mas) for a field star at 1 arcmin radius. The second is that the limiting magnitude for useful field stars increases sharply with aperture, provided the tilt sensor is built to sense the diffraction core of the star's laser-sharpened infrared image, rather than a seeing limited optical image.<sup>4</sup> Not only does the sharpness of the image compared to the seeing limit dramatically improve the sensitivity of the tilt measurement, but by enabling a sensor with pixels of very small angular subtense, the contamination by sky background can be reduced by many magnitudes. The limiting magnitude for tip-tilt sensing with the GMT is  $\geq 17$  in the H band, which is the key factor in realizing access

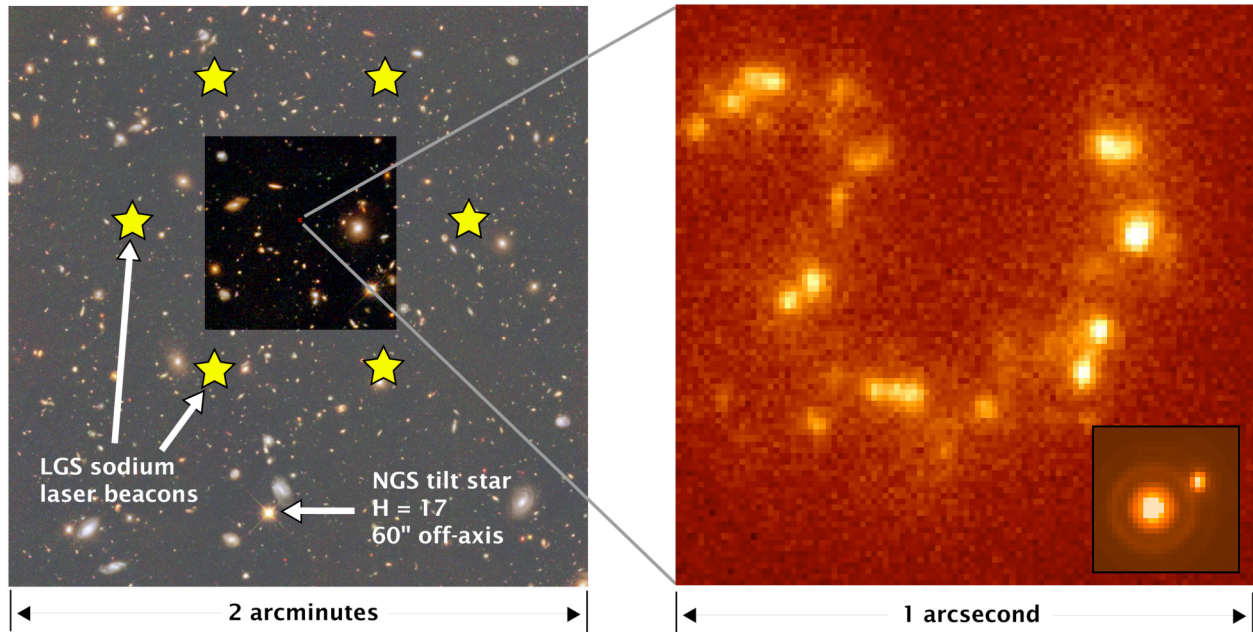


Figure 1. (*Left*) The 40 arcsec square field of the GMT HRCam imager is shown superposed on a deep 2 arcmin square NICMOS field from the HST. Simulated AO correction over this field is made from wavefront measurements of the six sodium laser beacons projected as shown at 35 arcsec radius, and an  $H = 17$  guide star 1 arcmin off axis. (*Right*) Detail of a 1 arcsec square within the corrected field showing a starburst galaxy at  $z = 1.4$ , as it would be detected in an H band image with the 17 mas resolution of the GMT AO system. Input was an  $H\alpha$  image of NGC 4038/39. The individual redshifted HII regions were taken to have H magnitude  $\sim 24.5$ . The detector plate scale is 10 mas/pixel. Sky noise is modeled for a 1 hour exposure through a 2.5% filter at the redshifted  $H\alpha$  wavelength. The insert shows the stellar PSF with the same 10 mas pixel size and the projected 40% Strehl ratio for two stars, one saturated, separated by 100 mas. The elongation is due to increased tilt anisoplanatism in the direction of the guide star.

to most of the sky. Taken together, the GMT with its multi-beacon system should be able to observe most scientific targets, with a contribution to the image width from uncontrolled jitter of only  $\sim 10$  mas RMS. This limit has helped us decide how aggressively we should set GMT goals for wavefront correction with the laser beacon system. The FWHM at the diffraction-limited point-spread function (PSF) of the GMT is 14 mas in H band, which would be increased to 17 mas by 10 mas of jitter. In the J band, 11 mas would be increased to 15 mas. Thus in terms of pushing the resolution limit for faint objects, we reach a point of diminishing returns around the H band.

The other key factor that must guide us is the corrected field of view. With a single deformable mirror this is limited because of anisoplanatism. The corrected field can be increased with multi-conjugate adaptive optics (MCAO), but even with just one deformable mirror, the field in the K band is already 25 arcsec in diameter, and often larger, 1300 times the diffraction width. The H band field of 18 arcsec is similarly rich. MCAO is therefore not included in the baseline design for GMT, though its inclusion in a future expansion is not precluded.

These considerations have led us to adopt for the GMT a baseline AO capability aimed at good correction in the H band. The target for wavefront accuracy is 200 nm RMS under typical seeing conditions. This is chosen to give good Strehl ratio in the H band, 56% for a tilt star on axis, degrading to 35% for a star 1 arcmin off axis. This goal is significantly better than is typically achieved with current systems, but our analysis shows it will be possible.

A second major goal for the GMT is extreme contrast adaptive optics (ExAO), for imaging other solar systems. In many cases the targets will be bright, consistent with the more accurate wavefront sensing and correction that will be essential for high contrast. Many targets with known planets are as bright as 6<sup>th</sup> magnitude, where we can aim at high Strehl ratio in the H band. Here, planet imaging to an inner working angle of  $4 \lambda/D$  (56 mas) is targeted, to allow detection in reflected light of many planets of known mass from radial velocity searches. Correction with AO to 112 nm RMS has been achieved in practice for a star of 6<sup>th</sup> magnitude in V.<sup>5</sup> For the GMT we set a target of 120 nm RMS error for such bright stars, corresponding to 80% Strehl at 1.65  $\mu\text{m}$ . Detection of thermal emission in the M band, where giant planets

are expected to be anomalously bright will also be important. Here 120 nm RMS corresponds to 98% Strehl ratio, a level that will allow high sensitivity to  $\sim 2 \lambda/D$ , or 84 mas radius.

The third goal for AO at the GMT is to improve seeing over a wide field by correction of just the ground layer (GLAO). This method is expected to give useful improvement in the H and K bands over fields up to 10 arcmin, and is planned for 8 m telescopes. While the GMT has no qualitative gain over an 8 m telescope in resolution in this mode, GLAO is needed to preserve its quantitative advantage of seven times higher throughput. The same laser beacons used for diffraction-limited imaging will also serve to implement GLAO simply by expanding the diameter of the beacon constellation and the projected pattern of the corresponding wavefront sensors. The large segment size of the GMT simplifies GLAO in that the individual 8 m apertures have diffraction limits much smaller than the near IR seeing and thus in this mode do not need to be coherently phased.

## 1.2. GMT AO challenges - special considerations for very large aperture

We recognize at the outset that our goals represent both a quantitative leap in resolution compared to present telescopes, as well as a qualitative leap in the art and technology of AO. The use of just a single LGS for wavefront sensing is a technique only now being exploited for scientific return. Tomographic wavefront sensing in closed loop with a constellation of several laser beacons is unproven at any telescope. Similarly, ground layer correction remains a plausible but still theoretical concept. Very high contrast imaging for exoplanet searches is also in its infancy. Thus we are faced with designing AO for a 25 m aperture with operational modes not yet fully developed even for an 8 m aperture. We examine here some specific issues peculiar to aberrations across very large apertures.

1. The amplitude of Kolmogorov turbulence increases as the 5/6 power of the aperture, while the wavefront error to reach a given Strehl ratio, after correction, remains independent of aperture. Therefore, there is a new challenge in dealing with unprecedentedly large aberrations of many  $\mu\text{m}$  over large scales. These aberrations must be measured and corrected to the same limit as small-scale errors. The outer scale of atmospheric turbulence may well be less than the 25 m aperture of the telescope and will provide some relief, but only under some conditions.
2. Wavefront aberrations generated in the telescope itself, from wind-induced vibrations and from local convection, are likely to be larger than for smaller telescopes that are lighter and stiffer unless great care is taken.
3. Wavefront discontinuities are present because of segmentation. Fortunately the advances made with the Keck telescope AO systems show that the difficulties presented by segmented primaries can be overcome.<sup>3</sup>
4. The diffraction limit for the thermal infrared for 25 m aperture becomes much sharper than the seeing limit. Current large aperture telescopes can be corrected in the 8-12  $\mu\text{m}$  region with a relatively simple tip-tilt secondary unless high dynamic range is important.<sup>6,7</sup> But for the GMT the larger aperture with full adaptive correction opens the possibility of greatly increased sensitivity in these thermal infrared bands, provided the advantage of sharper images is not offset by increased thermal background in the AO correction system.

To build a telescope that is to be at the forefront in AO not just ten years hence, but through the following decades, we need the clearest vision of both its potential as set by physical limits such as atmospheric turbulence and photon noise limited sensors, and also the engineering solutions that can exploit the advanced technology likely to be available then. Achieving the limiting capability for AO correction for the GMT, and indeed any ELT, will require a complex system. It follows that the AO system should, to the extent possible, not be duplicated for each instrument. A key challenge is therefore to incorporate all the AO correction and sensing elements into the telescope optical path, making the necessary separation of the beam for wavefront sensing without compromising the science instruments. Thus an overriding consideration in designing the GMT has been to try to anticipate these features and build them in.

## 2. DESIGN REQUIREMENTS

### 2.1. Adopted atmospheric parameters

As a baseline for quantifying the atmospheric disturbance and the performance of the AO systems in overcoming it, we have adopted values of the atmospheric parameters describing the spatial coherence  $r_0$ , temporal coherence  $\tau_0$ , and the isoplanatic angle  $\theta_0$ . In addition, an outer scale of turbulence  $L_0$  of 25 m has been assumed. These values have been derived from measurements from several sources: near-continuous night-time monitoring with MASS and DIMM instruments for the full year 2005 at both Cerro Las Campanas at the site of the 6.5 m Magellan telescopes and at Cerro

Tololo, and data from balloon flights conducted during the site testing campaign for Gemini South on Cerro Pachón. The values adopted are summarized in Table 1 below.

Table 1. Adopted values for key atmospheric parameters.

Parameter	0.5 $\mu\text{m}$			2.2 $\mu\text{m}$		
	Median	10 %ile	90 %ile	Median	10 %ile	90 %ile
$r_0$ (cm)	14.3	25.3	9.4	84.6	150	55.6
$\tau_0$ (ms)	2.07	3.51	0.79	12.2	20.8	4.7
$\theta_0$ (arcsec)*	2.10	2.80	1.33	12.4	16.6	7.9

\*Values of  $\theta_0$  at 2.2  $\mu\text{m}$  do not include the effect of outer scale, which will improve the size of the corrected field of view.

## 2.2. Requirements for diffraction-limited imaging

Performance targets are defined primarily in terms of residual wavefront error in the beam delivered by the telescope to AO instruments. The targeted wavefront errors are 200 nm RMS for general purpose LTAO observations, and 120 nm RMS for bright natural guide stars (NGS). These goals are better than typically achieved by current AO systems, but we project will be achievable with the GMT. The basis for this expectation comes from analysis of the component errors summarized in Section 2.6 which depend on many factors such as telescope aperture, laser power, and detector noise.

The AO system must hold a stable lock for up to an hour. Non-common path flexure, including the effect of slow guiding on a field star, must be held to no more than 3 mas over any  $5^\circ$  change of elevation angle to preserve image placement on a spectroscopic feed. All the sensing and control for performance at the required levels is to be built into the telescope. Dichroic and field mirrors will remove the light needed for wavefront sensing and segment phasing. The AO instruments will therefore need only a slow field star guider to remove effects of differential flexure.

We do not specify a field of view for the science imaging as a performance requirement, since we do not plan to implement MCAO for the initial system and the field is thus set by the prevailing atmospheric conditions.

## 2.3. Requirements for extreme contrast AO

The GMT will be used for direct detection of planets in two distinct wavelength regimes: 1.1-2.5  $\mu\text{m}$  (J, H, and K bands) and 3.5-5  $\mu\text{m}$  (L and M bands). In general, shorter wavelengths will allow imaging of planets fainter and closer to their parent star, but the diffraction limit advantage is offset by the difficulty of controlling residual wavefront phase errors and poor planet/star contrast for reflected light detections.

The two wavelength regions place different requirements on the performance of the AO system, but for both it is likely that scientific value will be greatest if the AO system will allow very high contrast within a few diffraction widths of the star. Only at these separations will it be possible to study a significant sample of planets of known mass from radial velocity, as well as to probe separations similar to giant planets in our own solar system. The wavefront corrections must be made so as to:

- 1) Reduce the RMS wavefront error, thereby maximizing the intensity of the exoplanet image.
- 2) Apodize the beam to suppress diffraction.
- 3) Minimize the noise in the averaged star halo in the search region.
- 4) Avoid aliasing and non-common path errors.

We set a requirement for 80% Strehl ratio for bright targets in the H band, which translates to 120 nm RMS wavefront error. This is driven mostly by the need to keep the planet signal as high as possible. The search region, where contrast is to be maximized, is taken to be an annular region around the star of inner radius  $4 \lambda/D$  and outer radius 0.6 arcsec.

## 2.4. Requirements for ground-layer AO

The requirement for GLAO is for correction over a field up to 8 arcmin diameter at the direct Gregorian focus. The target is for seeing reduction in the K band to 0.1 arcsec under good conditions (<0.4 arcsec seeing) and 0.25 arcsec under moderately poor conditions (0.7 arcsec). This requirement is somewhat uncertain at this stage, since GLAO has not yet been demonstrated in closed loop. However, uniquely among the AO modes planned for the telescope, GLAO is still fundamentally seeing limited, so its performance is essentially independent of the size of the aperture. In setting the requirement we have therefore appealed to the feasibility studies recently carried out for a GLAO system on the Gemini South telescope by Andersen et al.<sup>8</sup> and for the VLT by Hubin et al.<sup>9</sup>

## 2.5. Requirements for thermal performance

The thermal emissivity of the entire telescope and AO system must be less than 7%. This is set by the desire to take advantage of the low thermal background in those regions of the spectrum where sky is especially dark, for example, at 3.8  $\mu\text{m}$  and 11  $\mu\text{m}$ . In these regions the sky background is at or below that of a 3% emissive gray body. Even clean telescope optics are expected to contribute at approximately this level, and any unnecessary additional emissivity will result in additional observing time to reach the same sensitivity level.

The variable nature of the sky background in much of the thermal infrared places a requirement on rapid beam switching or chopping. The majority of observations will be of point sources ( $<1$  arcsec) where the chop should be significantly larger than the image size. We place a requirement of  $20 \lambda/D$  full throw at the longest wavelength of observation (25  $\mu\text{m}$ ), or a full chop throw of approximately 4 arcsec. This is within the range of the deformable secondary's actuators allowing implementation of chopping with the secondary, as is standard practice for thermal infrared observations.

The rate of chopping should be sufficient to minimize the noise contribution of the variable sky brightness. Our experience with the MMT AO system is that the sky does not vary at rates above 0.1 Hz on good nights. On nights which have thin clouds or high water vapor the sky variation can be both stronger and vary more rapidly. Thus the secondary should chop at least as fast as 1 Hz, with a goal of 5 Hz. The duty cycle should be 90% for this arrangement, requiring transition times of less than 50 ms and 10 ms for the requirement and goal rates respectively.

## 2.6. Summary of top-level AO system requirements

The performance requirements for the different AO modes are collected together in Table 2. Table 3 breaks out the major components of the wavefront error budget for the main AO modes.

# 3. SYSTEM ARCHITECTURE

The overall concept is shown schematically in Figure 2. The deformable Gregorian secondary, the beacon projector, and a removable artificial source are mounted at the top of the telescope. The lasers themselves are housed in a separate structure on the corotating azimuth platform. The optical and infrared wavefront sensing units are located on the upper side of the instrument platform above the direct focus, along with the diffraction-limited AO instruments. Instruments using GLAO are mounted below. The operation of the system is most readily understood by considering the four basic operational configurations, listed in Table 4. (ExAO is not included explicitly. It is treated as an extension of mode 3a.)

## 3.1. Correction with an adaptive secondary mirror

In order to meet the goals and challenges above, the GMT will base its AO system around a Gregorian deformable secondary mirror for wavefront correction. There are several advantages:

1. Deformable secondary technology has now matured to the point where it offers excellent overall performance in terms of high stroke and spatial resolution correction, fast response and accurate internal metrology.
2. Since all the telescope foci follow the secondary mirror, atmospheric correction at that mirror will be available for any instrument on the telescope which can benefit and for which wavefront information is available.
3. Sensitivity at wavelengths longward of  $\sim 2 \mu\text{m}$  is maximized because the correction is done without the addition of conventional warm reimaging optics, a tip-tilt mirror and a separate DM, all of which contribute thermal background. The deformable secondary mirror will allow diffraction-limited imaging with the highest sensitivity over the 2-25  $\mu\text{m}$  wavelength range where background emission from separate optics could otherwise dominate.
4. For ground layer correction there are two advantages. First, the field of view limitations from an optical relay are avoided. Second, the Gregorian deformable secondary conjugates to a height centered on the ground turbulence, 200 m above ground, for the widest possible field.

With such a powerful corrector built in, the goal of a universal wavefront sensing system becomes practical. The GMT deformable secondary will be built using the technology developed for the MMT and LBT secondaries.<sup>10,11</sup> It is specified to have 4620 actuators, the same number per 8 m segment as the LBT, and corresponding to a spacing of 32 cm at the entrance pupil. This enables a system with 120 nm RMS wavefront error as needed for ExAO at near and mid infrared wavelengths. It also opens the possibility of correction with useful Strehl ratio at wavelengths  $< 1 \mu\text{m}$ , where very high resolution imaging ( $\sim 7$  mas) around bright targets will be possible with CCDs.

Table 2. AO system requirement summary.

Component	Parameter	Requirement	Driver
System	Spectral range	0.9 – 25 $\mu\text{m}$	Science programs
	FOV transmitted to science instruments	1 arcmin 4 arcmin 8 arcmin	NIR Thermal IR GLAO
	Diffraction limited FOV	Not specified	Single conjugate correction
	Sky coverage	80% at 30° Galactic lat, 50% at pole anywhere >45° elevation	LTAO GLAO
	Lock hold max time	1 hour	NIR spectroscopy
	Flexure	3 mas over 5° elevation change	NIR spectroscopy
	Servo bandwidth	-3dB error rejection at 50 Hz	High Strehl ratio
	Emissivity increase	< 2 %	Thermal IR
	Segment phasing	< 50 nm RMS (Not required for GLAO)	High Strehl ratio
DM	Mirror type	Single adaptive secondary	
	Actuator spacing, count	32 cm at M1, 4620 total	High Strehl ratio
	Accuracy of control	Individual actuators to 5 nm RMS Fourier components to 0.26 nm RMS	High Strehl ratio ExAO
	Update rate	2000 Hz	ExAO
	Actuator stroke	150 $\mu\text{m}$	Chopping/windshake
	Full chop angle	4 arcsec	Thermal IR
	10%-90% chop time	8 ms (goal), 40 ms (requirement)	Thermal IR
LGS	Beacon type	Sodium resonance	Focal anisoplanatism
	Configuration	Six from 1.2 to 8 arcmin diameter	LTAO and GLAO
LGS WFS	Sensor type	Shack-Hartmann	
	Frame rate	1000 Hz	High Strehl ratio
	Total wavefront error	200 nm RMS	High Strehl ratio
Tilt sensor	Tilt sensor band	1-2.5 $\mu\text{m}$	Tilt sensitivity
	Sensor patrol field	2 arcmin radius	Sky coverage
	Tilt error	120 nm RMS	High Strehl ratio
NGS WFS	Sensor type	Shack-Hartmann with CCD Pyramid with NIR array	Classical AO IR science
	Frame rate	1000 Hz	High Strehl ratio
	Wavefront error	Shack-Hartmann: <200 nm RMS Pyramid: 120 nm RMS for H<6	Optical ExAO

Table 3. Main contributions to the AO corrected residual wavefront error.

Wavefront error source	RMS wavefront error (nm)		
	NGS	LTAO	ExAO
M1 figure	20	20	15
M2 figure	20	20	15
Piston anisoplanatism*	25	25	0
Piston from M1 edge sensors	25	25	25
AO optics (non-common path)	18	21	0
Science instrument	20	20	7
Fitting error	(49.4 cm subaps) 121	(49.4 cm subaps) 121	(32 cm subaps) 80
Atmospheric servo lag	(1 kHz read rate) 93	(1 kHz read rate) 93	(2 kHz read rate) 61
WFS measurement noise	( $m_V = 11$ ) 83	28	( $m_H = 6$ ) 50
Reconstruction error	52	95	0
<b>High order total</b>	<b>189</b>	<b>190</b>	<b>117</b>
Anisoplanatism error	All modes at 13": 260	Tilt at 1': 148	0
Residual windshake	50	50	30
<b>TOTAL</b>	<b>(Off axis) 325</b> <b>(On axis) 196</b>	<b>(Off axis) 246</b> <b>(On axis) 196</b>	<b>121</b>

\*Uncorrected errors in the mean phase between segments left by the NGS piston sensor as a result of anisoplanatism between the NGS and the on-axis science object, given for calibration error after 1 minute average at 60 arcsec radius (Section 3.6).

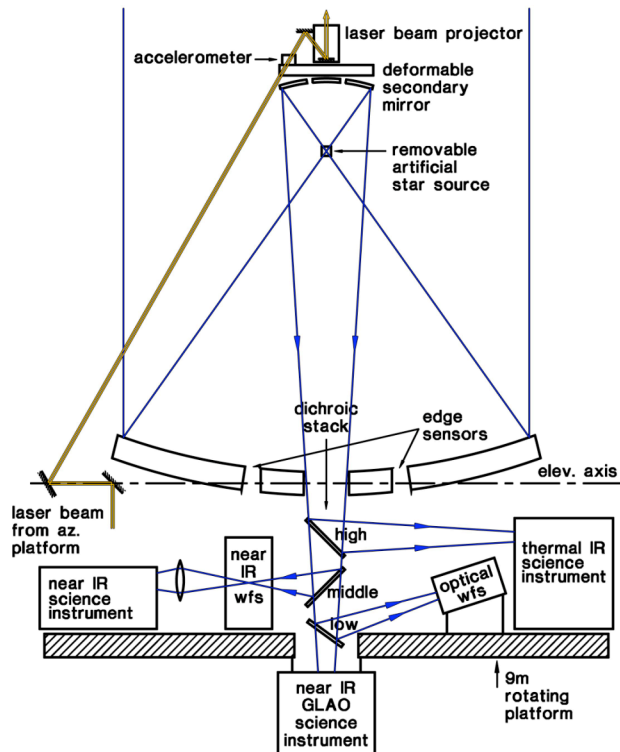


Figure 2. (Left) The AO system components mounted on the GMT telescope elevation structure (not to scale). Most of the science instruments and wavefront sensors remain fixed in place and are brought into play via a set of articulated, retractable dichroic mirrors marked low, middle and high. (Right) View showing the laser optics. Six sodium laser beacons are housed in the room on the az-platform (lower left). The beams are directed to a projector above the secondary via two flat mirrors on the elevation axis. The platform-mounted AO instruments are visible directly below the primary mirror assembly.

Table 4. Operational modes for the AO system. NIR = near infrared, PRWFS = pyramid wavefront sensor.

Operating mode	Science $\lambda$ ( $\mu\text{m}$ )	Focal station	Field (arcmin)	Dichroics: low-mid-high	Wavefront sensors	
					Fast tilt and piston	High order
1. No AO	-	Direct	24	out-out-out	-	-
		Folded	4			
2. GLAO	0.9-2.5	Direct	8	in-out-out	Optical NGS	LGS
3a. NIR NGS	0.9-2.5	Folded	1	in-in-out	NIR NGS	PRWFS
3b. NIR LTAO						LGS
4a. Thermal IR NGS	3-25	Folded	4	in-in-in	NIR NGS	PRWFS
4b. Thermal IR LTAO						LGS

### 3.2. A constellation of sodium LGS

To cover all the needs from narrow-field tomography to wide-field ground layer correction, a sodium beacon projection system will be built in to provide a constellation of variable diameter up to 8 arcmin. The diameter will be chosen according to the field to be corrected and the prevailing vertical distribution of aberrating layers. For narrow field tomography, the diameter will be 1.2 arcmin, so that their light collectively samples the full volume of atmosphere traversed by light from a target on axis. The instantaneous stellar wavefront will be computed by a tomographic algorithm applied to the wavefronts measured from all the beacons.<sup>12-14</sup> While in the first light configuration correction will be made with the adaptive secondary alone, the tomographic method will yield the information needed to implement MCAO for wider field. Thus, the groundwork is laid for this addition at a later stage.

Six beacons will be projected in a regular hexagon. This number is favorable for tomography, and also for the reduction of interference of the Rayleigh scattered column of one laser with the resonance beacon of another (fratricide). This is markedly reduced if the beacons are projected in the directions of the six gaps, as shown in Figure 3. Continuous wave (CW) sodium lasers of 30 W each will be used, based on the existing summed frequency YAG technology demonstrated for guide stars at the Starfire Optical Range.<sup>15</sup>

### 3.3. Lasers and beam projector

The lasers that generate the LGS will be housed in a thermally isolated enclosure on the azimuth platform. The beam path runs from the top of the enclosure to the elevation axis, and thence to the beam projector telescope behind the secondary mirror. The short jog along the elevation axis is done with two mirrors. The first is articulated, driven as the telescope moves in elevation to remain fixed with respect to the lasers. The second mirror is mounted rigidly to the telescope. In this way, the laser beam pointing remains coaxial as the telescope tracks.

The lasers themselves will be mounted vertically against the inside wall of the enclosure, with electronics and closed-cycle coolers mounted against the outer wall. The six beams, projected upward, are routed across the ceiling by mirrors, and arranged in the final hexagonal pattern of variable radius. Lasers meeting the power requirement are only now being realized, and their native polarization is likely to be linear. On the other hand, maximum return from the sodium layer is achieved with circular polarization because of optical pumping of the sodium atoms. Adjustable phase plates will therefore be included in the six beams, with rotation controlled by a sensor mounted in the beam just before the last lens of the projector to maintain circularity at the exit pupil as the telescope moves in elevation.

The optical design puts 13 reflective and 8 refractive surfaces between the laser heads and the sky. With efficient coatings and a moderate amount of dust accumulation, we anticipate a loss of 2% per surface or 65% overall throughput.

### 3.4. Wavefront sensing with the LGS

Beacon light will be recorded by Shack-Hartmann sensors, one per beacon, with 17 square subapertures across each 8.4 m segment. This yields a total of 1540 subapertures with >50% illumination. Of these, 4 beacons lose 115 to fratricide, and 2 beacons lose 132. Each Shack-Hartmann pattern will be imaged on a 256x256 pixel CCD, with a 5x5 region devoted to each subaperture, configured as a 4x4 cell with a single-pixel guard band. Each subaperture of the lenslet arrays will be an anamorphic lens designed to compress the radially elongated LGS image down to a circular image. While this will not recover the sensitivity lost in the direction of the elongation, it will minimize the number of pixels and the read noise included in the slope calculations. The CCDs will need between 64 and 256 separate readout amplifiers running in parallel to achieve the required 1 kHz frame rate with 3 e- read noise.

### 3.5. Sensing low-frequency modes with starlight

As has been found at the Keck II telescope, drift of the LGS sensors and unknown variations in the height of the sodium layer mean that periodic calibration against a slow NGS sensor is essential. Optical light from a field star will be used, transmitted to a separate Shack-Hartmann sensor that will use the same subaperture configuration as the LGS sensors. A table of centroid offsets in the LGS real-time slope calculator and the axial positions of the WFS themselves will be updated with information from this sensor. Depending on the brightness of the NGS and the time needed to average out anisoplanatism, updates from it will be computed on a timescale of tens of seconds.

The infrared wavefront of a natural guide star corrected by LTAO is coherent across the full aperture, allowing direct sensing to high accuracy of the modes of lowest spatial frequency. For the GMT, global tilt sensing will be from the IR image of the same field star used for LGS calibration, reflected to the IR wavefront sensor unit. The infrared advantage

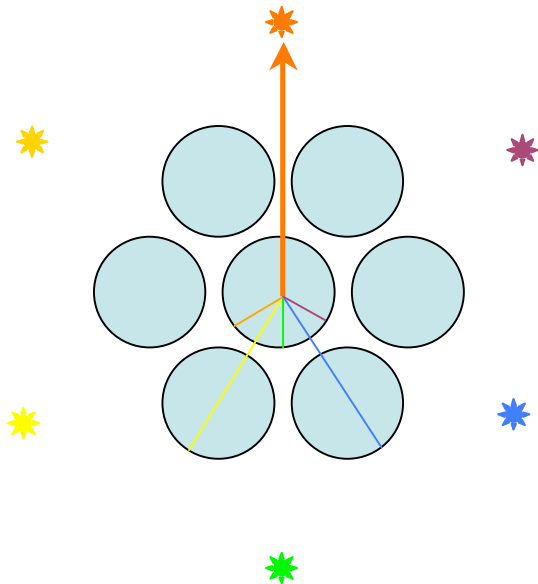


Figure 3. Pattern of potential fratricide for the WFS looking at the top beacon. Subapertures lying in the “shadow” cast by the top beacon of the Rayleigh columns from the other 5 beams see Rayleigh light in addition to the resonance light and will be unusable. The affected regions of the pupil are shown as radial lines.



increases for very large telescopes since not only does the image become sharper, but the flux in the image increases. Furthermore, the increase in image sharpness with larger aperture reduces the noise from underlying sky background because smaller sensor pixels may be used. Thus for a guide star at  $H = 17$  at 20% Strehl ratio, the diffraction core surface brightness is  $\sim 10^{\text{th}}$  mag/arcsec, still  $15\times$  brighter than sky background of  $H = 13$  per square arcsec.

### 3.6. Inter-segment piston control

For all segmented mirrors the absolute wavefront steps across the gaps between the segments must be measured and periodically calibrated by interferometry from a natural star. Because the full pupil has only seven segments, the NGS piston measurement could be recovered at high speed and high accuracy for even quite faint guide stars on-axis. Nevertheless, anisoplanatism will limit the value of such sensing in the general LTAO case. Thus we adopt an approach similar to the high-order correction: fast measurement sensors supplemented by periodic calibration.

Most of the atmospheric piston error will be removed by interpolating the Shack-Hartmann data in the lowest spatial frequency modes across the 30 cm gaps. But these sensors cannot help with primary segment piston displacements induced by wind buffeting and vibration. Instead, edge sensors will bridge the gaps between the segments optically to recover these errors with 20 nm accuracy and high speed. Fast correction will be by the secondary mirror segments, while the error build-up will be offloaded to the primary mirror actuators on a time scale of minutes.

Periodic absolute calibration will be made with a small fraction of the near IR NGS starlight forming two defocused images on a separate small detector array built into each tilt sensor. These images will be read out about once a minute, and a phase-diversity algorithm will recover the six long-term average relative piston errors from the image pair.

### 3.7. Wavefront sensing with NGS

The classic NGS AO mode will be available, without lasers, when an adequately bright natural star is available for the science program. In the case of exoplanet searches when the primary star is bright it will always be the wavefront reference. Two NGS wavefront sensors will be provided. The visible Shack-Hartmann sensor normally deployed as the low bandwidth corrector for the LGS sensors may be used also at high speed, offering a conventional NGS capability with 0.49 m subapertures, and for magnitudes  $V < 11$  is expected to outperform LTAO. Also available will be a near IR pyramid sensor (PRWFS) in the same area as the near IR tilt and piston sensors. With scalable subaperture size down to 0.32 m, it will be sensitive over a range of guide star brightness. Anticipating the availability of low noise IR array detectors, the PRWFS is likely to be the preferred NGS sensor except when near IR science requirements preclude its use, because of its inherently higher accuracy determination of low-order modes than the Shack-Hartmann sensor.

### 3.8. Wavefront sensing for ExAO

We briefly summarize here the strategy for high fidelity wavefront sensing. A fuller discussion is presented by Angel et al.<sup>2</sup> For high contrast imaging close to a stellar core, apodization is needed to suppress diffraction. Conventional Lyot coronagraphy is inefficient, because strong suppression results in substantial loss of both flux and resolution. This is especially true for the GMT pupil. However, efficient apodization of the GMT is possible by introducing a static phase aberration across the pupil. The effect is to modify the PSF, moving energy from one side to the other. The correction is chromatic, but for 5% bandwidth can be very effective with suppression to  $10^{-6}$  from 4 to  $10 \lambda/D$ . GMT's ExAO instrument will implement several 5% bandwidth channels simultaneously, separated by dichroic mirrors.

The residual stellar halo in the search region must be both as faint and smooth as possible. Speckle structure must therefore be actively and immediately suppressed. We expect to accomplish this with focal plane interferometric sensors to measure the complex amplitude of the instantaneous halo directly, thus removing all non-common-path errors. Corrections will be fed back to the adaptive secondary. This will require use of small arrays of single photon counting IR detectors which are now no more than a few years away.

### 3.9. Wavefront reconstruction

The size of the computational problem in calculating the commands to the DM's 4620 actuators is challenging. With the LGS in operation, the Shack-Hartmann sensor for each of the six beacons has approximately 1500 subapertures. The reconstructor matrix would then naively have  $17032 \times 4620$  elements. On each iteration, wavefront reconstruction with a fully-populated matrix would require  $8 \times 10^7$  floating point operations. The real-time computer would have to be capable of sustained calculation at a minimum of 100 GFlop.

For the GMT, though, there is no coupling of actuator influences across the segment boundaries. The wavefront reconstruction can be conceptually broken into two pieces: the first recovers the 8.4 m pieces of wavefront across each of the segments independently, and the second estimates those few low-order modes across the full 24.4 m pupil that contribute significantly to the atmospheric piston errors. The computational demand is therefore reduced by a factor of seven, since actuators on a given secondary segment are driven almost entirely by Shack-Hartmann slopes measured within the same segment. In fact, each segment needs less computing power than the planned Gemini MCAO system,<sup>16</sup> which will drive three DMs (instead of one) from five laser beacons sensed with about the same pupil sampling as GMT.

The real-time computer must run at ~15 GFlop sustained throughput, which would not be particularly difficult to construct even today. The MMT tomographic system will be driven by a computer built by Microgate, which is designed to accept up to 1500 WFS slope inputs, and drive the MMT's 336-actuator ASM at 1 kHz frame rate. It is capable of sustained calculation at ~1 GFlop, and is a small unit, easily fitting into a single bay of a standard 19 inch rack. It is designed around custom boards, with computation handled by floating point DSPs, and high-speed communication handled by large FPGAs. It is a readily expandable architecture which we adopt for GMT, anticipating that it will be implemented with upgraded hardware to be expected on the timescale of the telescope's construction.

### 3.10. Closed loop operation

Each of the GMT's seven primary and corresponding secondary segments can be considered as an 8 m AO system in its own right, with its own deformable secondary and a six-beacon laser constellation for wavefront sensing. When the AO system is turned on, and before any segment co-phasing has been implemented, each segment is expected to perform at the levels projected for 8 m class telescopes with advanced AO systems. The analysis and experience being developed with monolithic primary mirrors at such telescopes will all be directly applicable to the individual GMT segments. The remaining task is to control the piston errors across the segment gaps to high accuracy. This will be done as follows:

*Static set up.* Set the secondary segments so they form a continuous surface, using optical metrology with the artificial light source. Use the starlight piston sensor to measure the telescope segment displacements, and remove them by adjusting the primary segments so speckles are seen in white light.

*Low frequency control.* The primary segment edge sensors will measure differential motions due to telescope structural deformation. Such deformation will be caused by wind gusting on a time scale of seconds; changing elevation and thermal distortions will cause larger but slower changes. These will be corrected on short time scales with compensating secondary motions, and by readjusting the primary segments at longer intervals (several minutes).

*Fast control (kHz).* Corrections to the wavefront shape including tilt and piston terms interpolated across the gaps are sensed at kHz rates optically by the Shack-Hartmann reconstruction and tilt sensors and mechanically by accelerometers. The adaptive secondary segments will be adjusted to compensate these fast changes. The commands to each segment will include piston motions to ensure continuity of the corrected wavefront across the boundaries.

The wavefront errors to be controlled can be divided into high order errors from atmospheric turbulence, global tilt errors from the atmosphere, vibration, and wind buffet, and piston errors between the segments from all sources. All these errors must be controlled

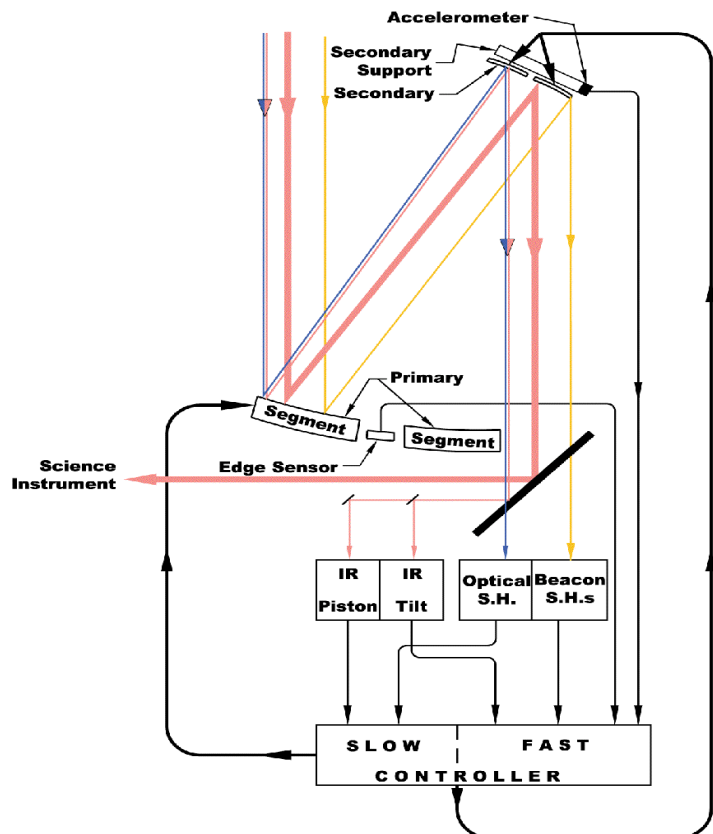


Figure 4. Overview of the wavefront control paths for GMT. The thick black line at 45° represents the middle dichroic of Figure 2, transmitting the laser and visible starlight and reflecting the near infrared.

to high accuracy in all AO modes, with the exception of inter-segment piston errors in the case of GLAO. The most general case is control to the diffraction limit using LTAO, which uses most of the hardware elements of the AO system. The overall control strategy for this mode of operation is shown in Figure 4.

### 3.11. Instrument layout

A plan view of the instrument configuration on the telescope's instrument rotator platform is shown in Figure 5. The near infrared beam for instruments and WFSs operating in the JHK bands is reflected to the left out of the main beam by the middle dichroic which transmits optical light through to the low dichroic and optical WFS. At the bent Gregorian focus the tilt star will be accessed by one of three field probes to feed the IR sensors that measure phase steps between the seven segments, global image motion at full speed, and focus shifts arising from changes in the height of the sodium layer, none of which are well sensed by the lasers. In addition the infrared pyramid sensor is housed here, fed either by a small probe mirror or, to access an on-axis bright target, by a dichroic with one of the J, H or K bands.

The full suite of optical and IR sensors can be used to correct for science instruments both in the JHK bands, which will access the 1 arcmin field passing the sensors and corrected by an Offner relay (mode 3), shown in Figure 6, and in longer thermal bands, feed a 4 arcmin field by reflection from the high dichroic brought in above, transmitting both optical and near infrared through to the sensors (mode 4). To maintain diffraction limited imaging performance when the upper dichroic is in place, aberrations in the transmitted beam will be corrected by a compensating plate inserted ahead of the near IR focus. In all cases the science beam will be correctable either by tomography with the LGS, or by a natural star.

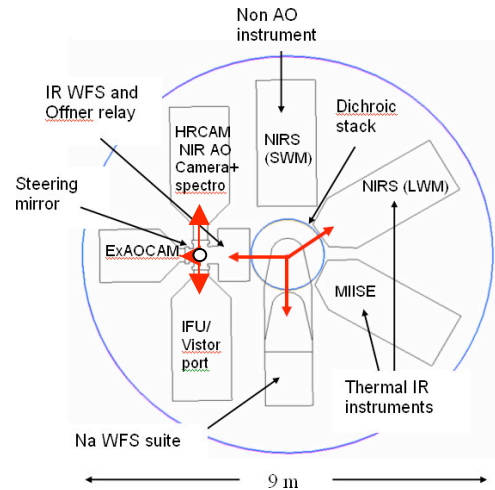


Figure 5. Schematic plan view of the instrument platform. The thick red arrows show three simultaneous beams going from the low dichroic to the optical sensor (6 o'clock), from the mid-dichroic to the near IR WFS, Offner relay and instrument (9 o'clock) and from the high dichroic to a thermal IR instrument (2 o'clock). HRCAM provides 1-2.5  $\mu\text{m}$  AO imaging and long slit spectra. The ExAO CAM allows very high-contrast NIR imaging. NIRS provides high resolution spectroscopy from 1-2.5  $\mu\text{m}$  (SWM) and 3-5  $\mu\text{m}$  (LWM). MIISE provides 3-25  $\mu\text{m}$  imaging, spectra, and nulling interferometry.

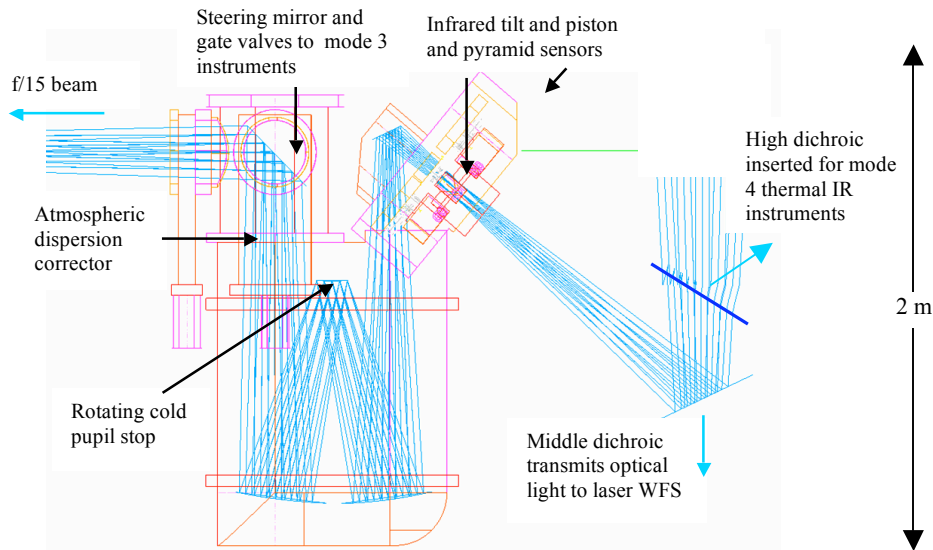


Figure 6. Configurations for modes 3 and 4, IR diffraction limited imaging (view rotated 90 degrees from Figure 5). The beam over 1-2.5  $\mu\text{m}$  is reflected to the left off the mid dichroic, while transmitting the optical beam through to the lower dichroic and optical wavefront sensors. This beam enters the dewar before the focus. The infrared sensors deploy across a 4 arcmin field, and a 1 arcmin field passes through to the modified Offner relay which yields an f/15 beam. This passes through an atmospheric dispersion corrector up to a beam steering mirror to the instruments, which are connected by gate valves.

## 4. CONCLUSIONS

The design of the AO systems for GMT is aimed at achieving the three goals of diffraction-limited near-IR imaging over most of the sky, wide-field ground-layer correction, and very high contrast AO for faint companion detection. A key design principle has been to build the system around common essential components, to minimize system complexity and cost. In this spirit, an adaptive secondary mirror is used as the wavefront corrector and a suite of sodium LGS and WFS does most of the wavefront sensing. Use of an adaptive secondary with segments matched to those of the primary confers substantial additional benefits: the cleanest thermal environment is maintained while preserving étendue for GLAO. In addition, the agile secondary segments can rapidly respond to motions of the primary segments induced by wind buffet or vibration.

MCAO is not included as a baseline mode because we project that the great majority of the sky will be reachable with LTAO alone. The LGS and a single tilt star within 1 arcmin of the science target should give wavefront measurements of sufficient fidelity to recover H band Strehl ratio of >35%. Coverage will be 50% at the Galactic pole, increasing to 80% at 30° latitude.

## 5. ACKNOWLEDGEMENTS

We are grateful for the support and valuable contributions from the GMT Project Scientists Working Group, in particular Matt Johns, Steve Shectman, Dan Fabricant, and Paul Schechter. The work has been supported by the NSF under grant AST-0138347.

## 6. REFERENCES

1. M. Johns, "The Giant Magellan Telescope (GMT)," in *Ground-Based and Airborne Telescopes*, (Proc. SPIE), ed. L. M. Stepp, **6267**, (2006).
2. J. R. P. Angel, J. L. Codona, P. M. Hinz, and L. M. Close, "Exoplanet imaging with the Giant Magellan Telescope," in *Ground-Based and Airborne Telescopes*, (Proc. SPIE), ed. L. M. Stepp, **6267**, (2006).
3. P. L. Wizinowich et al., "Adaptive optics developments at Keck Observatory," in *Advancements in Adaptive Optics*, (Proc. SPIE), eds. D. Bonaccini, B. L. Ellerbroek, & R. Ragazzoni, **5490**, 1 (2004).
4. J. R. P. Angel, "Use of natural stars with laser beacons for large telescope adaptive optics," Proc. Laser Guide Star Adaptive Optics Workshop, Kirtland AFB, Albuquerque, **2**, 494, (1992).
5. R. Q. Fugate et al., "Adaptive Optics for the 21<sup>st</sup> Century," ASP Conference Series, **174**, 55 (1999).
6. L. M. Close et al., "Mid-infrared imaging of the post-AGB star AC Herculis with the MMT adaptive optics system," *ApJ Lett*, **598**, L35 (2003).
7. W. M. Liu et al., "Resolved mid-infrared emission around AB Aurigae and V892 Tauri with adaptive optics nulling interferometric observations," *ApJ Lett*, **618**, L133 (2005).
8. D. R. Andersen et al., "Modeling a GLAO system for the Gemini Observatory," these proceedings.
9. N. Hubin, M. Le Louarn, R. Conzelmann, B. Delabre, E. Fedrigo, & R. Stuik, "Ground layer AO correction for the VLT MUSE project," in *Advancements in Adaptive Optics*, (Proc. SPIE), eds. D. Bonaccini, B. L. Ellerbroek, & R. Ragazzoni, **5490**, 846 (2004).
10. F. Wildi, G. Brusa, M. Lloyd-Hart, L. Close, and A. Riccardi, "First light of the 6.5-m MMT adaptive optics system," in *Astronomical Adaptive Optics Systems and Applications*, (Proc. SPIE), eds. R. K. Tyson & M. Lloyd-Hart, **5169**, 17 (2003).
11. A. Riccardi et al., "Adaptive secondary mirrors for the Large Binocular Telescope", in *Astronomical Adaptive Optics Systems and Applications*, (Proc. SPIE), eds. R. K. Tyson & M. Lloyd-Hart, (Proc. SPIE) **5169**, 159 (2003).
12. R. Ragazzoni, E. Marchetti, & F. Rigaut, "Modal tomography for adaptive optics," *A&A Lett.*, **342**, L53 (1999).
13. A. Tokovinin, M. Le Louarn, E. Viard, N. Hubin, N., & R. Conan, "Optimized Modal Tomography in Adaptive Optics," *A&A*, **378**, 710 (2001).
14. M. Lloyd-Hart & N. M. Milton, "Fundamental limits on isoplanatic correction with multiconjugate adaptive optics," *JOSA A*, **20**, 1949 (2003).
15. R. Q. Fugate et al., "Progress toward a 50-watt facility-class sodium guide star pump laser," in *Advancements in Adaptive Optics*, (Proc. SPIE), eds. D. Bonaccini, B. L. Ellerbroek, & R. Ragazzoni, **5490**, 1010 (2004).
16. B. L. Ellerbroek et al., "MCAO for Gemini-South," in *Adaptive Optical System Technologies II*, (Proc. SPIE), eds. P. L. Wizinowich & D. Bonaccini, **4839**, 55 (2003).